International Journal of Thermal Sciences 159 (2021) 106594

Contents lists available at ScienceDirect

International Journal of Thermal Sciences

journal homepage: http://www.elsevier.com/locate/ijts

The effect of ethylene glycol concentration on the interfacial dynamics of the successive droplets impacting onto a horizontal hot solid surface

Teguh Wibowo [a,c], Arif Widyatama [a,b], Samsul Kamal [a,b], Indarto [a,b], Deendarlianto [a,b,*]

[a] Department of Mechanical & Industrial Engineering, Faculty of Engineering, Gadjah Mada University, Jalan Grafika No.2, Yogyakarta, 55281, Indonesia
[b] Center for Energy Studies, Gadjah Mada University, Sekip Blok K 1A, Kampus UGM, Bulaksumur, Yogyakarta, 55281, Indonesia
[c] Department of Mechanical Engineering, Sekolah Tinggi Teknologi Adisutjipto, Jl. Janti Blok R. Lanud, Yogyakarta, 55198, Indonesia

ARTICLE INFO

Keywords:
Spray cooling
Successive droplets
Spreading ratio
Apex height

ABSTRACT

The present work aimed to conduct the visualization study on the effect of the ethylene glycol concentration on the interfacial behavior of successive droplets during the impacting onto a horizontal hot solid surface. The tested liquid droplets were pure water and two ethylene glycol-water mixtures, which contain 10% and 20% of ethylene glycol. A polished cylindrical plate of stainless steel (SUS 304), with the surface roughness of 0.06 μm, was utilized as a solid surface. The surface varies for temperatures of about 110 °C–240 °C. The detailed phenomena during the droplet impact were recorded by using a high-speed video camera with the frame speed of 2000 fps and the resolution of the 1024 × 768. In addition, an own developed image processing technique was also implemented to obtain the quantitative parameters, such as the spreading ratio and the apex height during the droplet impacting onto a hot solid surface. As a result, the interfacial dynamics of the successive droplets were clarified. The addition of the concentration of ethylene glycol leads to the decrease of droplet oscillation during the spreading phase and delays both the bubble formation and the presence of secondary droplets. In addition, the research also reveals that the presence of the second droplet successfully improves the wetting area of the droplet.

1. Introduction

The cooling system utilizing liquid media becomes a critical part of various industry, especially the metal industry, which work under high temperature. For instance, the quenching process of metal is essentially needed to achieve the desired metal structure as well as improve the material properties such as strength and hardness. Because of the benefits, spray cooling becomes one of the suitable methods in metal cooling. The main advantages of this method were realized by previous researchers, such as Deendarlianto et al. [1], who concluded that the heat fluxes produced by liquid droplet impacting onto a hot surface are much higher than that of the forced convective cooling. Equally important, the spray cooling is also widely known due to its adaption ability in various cooling situations as well as savings inflow rate requirements [2]. In the industrial applications, the liquid agent distribution contributes to the formation of many droplets that is difficult to study systematically under realistic conditions [3]. For this reason, single droplet experiments can be used to understand the transient heat transfer features required to predict the overall heat transfer property of an overall spray. Several methods have been developed to fulfill the importance of each relation aspect, and the spray cooling had shown its effectiveness as a thermal control [4].

Besides the application of spray cooling, the liquid droplet can be widely implemented in other fields of works, such as in the combustion process of liquid fuel [5], the inkjet technology in the printing system [6], and spray coating [7]. In addition, several studies have focused on the impingement on heated surfaces of water droplets containing additives [8–10]. Those widespread applications indicate that comprehensive knowledge is essentially needed since the desired effect may vary according to the application [11]. A fundamental understanding of droplet interfacial dynamics is also crucial to handle some controllable parameters during the operation process, such as wettability, impact speed, and surface temperature [12]. For instance, the parameter of surface temperature should consider the Leidenfrost phenomenon, which strongly influences the heat transfer performance. It is described as the presence of a thin vapor layer, which prevents the contact between liquid droplets and the hot surface. The research conducted by Chandra and Avedisian [13] pointed out the importance of Leidenfrost

* Corresponding author. Department of Mechanical and Industrial Engineering, Faculty of Engineering, Gadjah Mada University, Indonesia.
E-mail address: deendarlianto@ugm.ac.id (Deendarlianto).

https://doi.org/10.1016/j.ijthermalsci.2020.106594
Received 27 June 2019; Received in revised form 6 February 2020; Accepted 19 August 2020
Available online 25 August 2020
1290-0729/

point, producing the longest evaporation time and the lowest high transfer rate.

Boiling is defined as the phase transformation from liquid to vapor under a particular condition. In the phenomenon of a droplet impacting the hot surface, the boiling process occurs when the liquid droplet is in contact with the solid surface where the surface temperature is maintained above the saturation temperature of the liquid. Liang and Mudawar [14] classified those boiling phenomena regimes according to the wall temperatures and evaporation behavior. The regimes are film evaporation, nucleate boiling, transition boiling, and film boiling. Moreover, Bernardin et al. [2] reported that the regimes of a droplet impacting hot surfaces are strongly affected by surface temperature and Weber number. The detailed observation of the evaporation characteristics and droplet break up event was also conducted by Ko and Chung [15]. To conclude, the above studies reveal that each regime experiences different mechanisms and strongly influences the heat transfer process and fluid flow. Therefore, an in-depth analysis of these aspects has attracted researcher attention [16].

In general, the phenomenon of a liquid droplet impacting onto hot solid surfaces can be explained as follows. As the droplet comes out from the droplet generator and hits a hot surface, it experiences the change of movement direction. The kinetic energy in the droplet body is released into the radial direction. After reaching the maximum spreading diameter, the droplet retracts back under the action of surface tension [17] and produces a complex phenomenon. Each case produces a different behavior since it is influenced by many factors such as droplet diameter [18,19], the fluid properties [20–22], the surface roughness [23–25], and the surface material [26,27].

The recent study is even expanded into a more complex matter since both in nature and industrial application, the occurred phenomena are certainly more complicated than that of the impact of a single droplet. Most of the droplets act in the form of successive droplets, which means the interaction between droplets should be considered in the analysis. Fujimoto et al. [28] argued that the fundamental understanding during the successive droplets impinging onto a hot solid surface requires extensive investigations. Several comprehensive researches on the successive droplets have been conducted by previous researchers [28–32] to gather droplet characteristics. In terms of experiments, Fujimoto et al. [33] utilized two-directional photography to capture the phenomena of two successive water droplets impacting Inconel alloy and successfully discussed the droplet collision as well as the effect of the spacing between the two droplets.

Furthermore, numerical investigation, covering volume-of-fluid to determine the free liquid of surface and continuum surface force model to calculate the surface tension, were conducted by Tong et al. [34]. They successfully obtained the detailed flow fields of the liquid and provide the physics during the impingement. Kuznetsov et al. [35] concluded that the kinetic energy acting in the radial direction transforms into the viscous dissipation energy, while the initial kinetic energy of the droplet partially transforms into the surface tension energy and viscous dissipation energy. However, the available research related to successive droplet has not revealed all phenomena, especially the phenomena which can only be analyzed from high-quality data. At the same time, the recent trend research proves that the image processing technique has become a reliable method to enrich the analysis process. Hence, it is important to carry-out more experimental works, mainly utilizing image processing techniques, in order to reveal the comprehensive behavior of successive droplets impacting onto a hot solid surface.

Although the water is still considered as the most favorite liquid for spray cooling, it is also essential to find a proper method to enhance the cooling performance of the droplet by adding the surfactant or other liquid to form a solution. Cui et al. [9] compared three kinds of salts (NaCl, Na_2SO_4, and $MgSO_4$) on metal cooling behavior. They mentioned that each salt produces a particular effect on the various parameter such as nucleate boiling heat transfer and boiling transition. Clay and Miskis [36] investigated the effect of surfactant on the droplet spreading, and concluded that the increase of the surfactant decreases the spreading rate of the droplet due to the formation of a negative surface tension gradients near the contact line. Next, Pontes et al. [37] performed the experiments to examine the effect of the ethanol-water solution on the single droplet impacting onto a hot solid surface. They reported that the ethanol-water solution reaches the maximum spreading diameter slightly faster than the water. In addition, the spreading diameter of the ethanol solution was larger than that of the water. Although the importance of the effect of the physical properties on the droplet behavior was examined by previous researchers, a complete understanding of it has not achieved yet. Therefore, the droplet dynamics should be deeply investigated to obtain more detailed information, such as the entrainment of the small bubble, and explain how the change of fluid properties affects the droplet dynamics.

From the above facts, it was concluded that most of the researches were conducted in the form of single droplet impact conditions, whereas in the practical application, the multiple successive droplets were often found. In addition, it is also noticed that a comprehensive study on the effect of fluid properties is rarely discussed. On the other hand, in the cooling and conventional heat exchanger system, several additives have been used to improve the properties of a liquid, such as the freezing point and boiling point of the ethylene glycol. In general, the recent research of ethylene glycol utilization is still focused on the radiator system [38], whereas the comprehensive research on the spray cooling, as well as multiple droplets behavior, was not been conducted. Therefore, the present research will increase the understanding of the physical phenomena of ethylene glycol droplets on spray cooling.

The present experimental study aims to investigate the effect of the concentration of ethylene glycol in a water solution on the interfacial dynamics during the successive droplets impacting onto a hot solid surface. For that reason, the pure water and the ethylene glycol-water mixture were used as the working fluids. The surface temperature was achieved by using an induction heater. Next, the own developed image processing technique was implemented to gather the main quantitative parameters from the video images obtained from the experiments. The use of high-speed video camera, up to 2000fps, that was combined with the application of image processing technique, allowed this work to produce useful data and conduct in-depth analysis. Hence, the results revealed the comprehension phenomena of droplets impacting onto a hot surface. Finally, the present work provides more detailed information on the interfacial characteristics of successive droplets, in terms of the properties of fluid dependence on related phenomena experimentally.

2. Experimental apparatus and procedures

The schematic diagram of the experimental apparatus in the present experimental study is shown in Fig. 1. The apparatus consists of a solid surface, an induction heater, a droplet generator to produce the successive droplets, a high-speed video camera, and an illumination system to capture the detailed image of the droplets.

The droplet generator consists of droplet injector and the fluid tank. The droplet injector was used to inject the droplets to the surface at 50 mm above the hot surface. In the present work, the diameter and the frequency of the droplet were 3.12 mm and 8.5 droplets per second, respectively.

In the present experimental work, an induction heater, as shown clearly in Fig. 2 was used as a heat source. The main parts of the induction heater are a large copper coil, power supply, controller, and a cooling fan. The hot surface used in the present experiment was polished stainless steel (SUS 304). The surface roughness was Ra = 0.06 μm, as shown in Fig. 3. The temperature was monitored using a K-type thermocouple. Three thermocouples were placed in a specific place on the surface to ensure the surface temperature can be measured accurately.

The present experimental study is mainly designed to reveal the

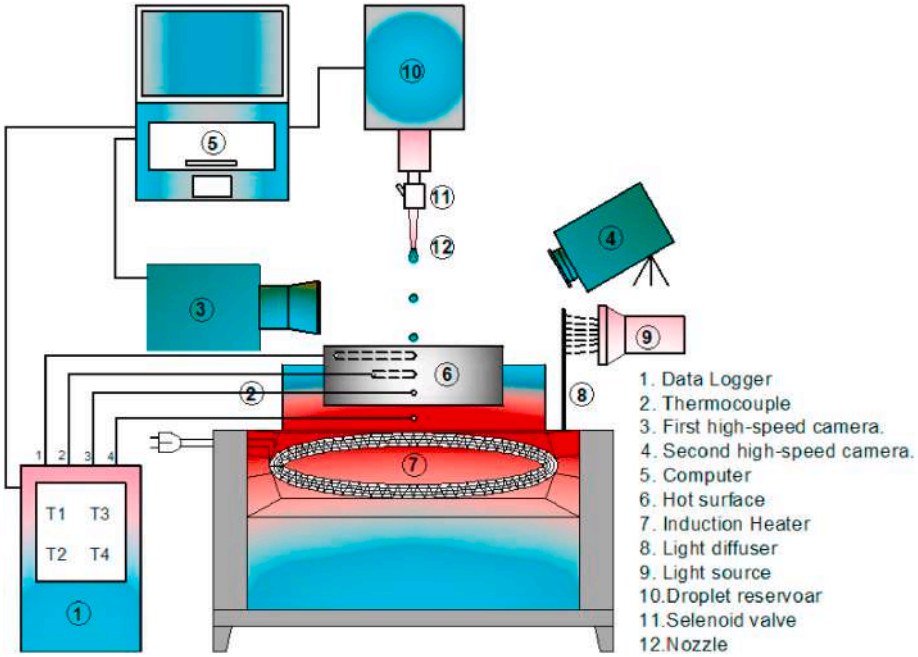

Fig. 1. The schematic diagram of the experimental apparatus.

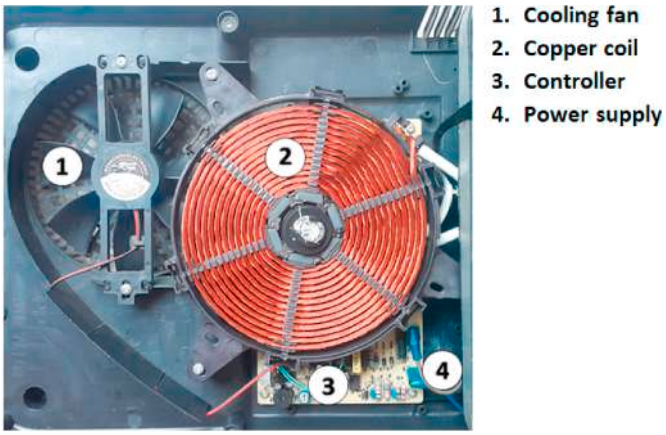

Fig. 2. Inside view of the induction heater used in the experiment.

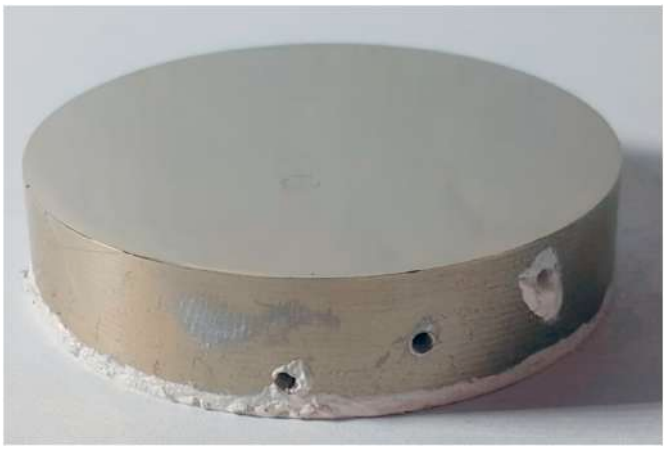

Fig. 3. The stainless steel material.

effect of ethylene glycol addition on the multiple droplet behavior. Hence, three different liquid was utilized. The first liquid was pure water, which is denoted as 0 EG. In addition, two other solutions contain 10% and 20% ethylene glycol were also used, and those are denoted as 10 EG and 20 EG, respectively. Furthermore, the addition of ethylene glycol also affects the properties of the fluid. Each property of fluid was tested, and the summarize of the properties is listed in Table 1. Equally important, the dimensionless parameters of each working fluids are also determined, as shown in Table 2. Re, We, and Oh, in the table, derive the Reynolds, Weber, and Ohnesorge numbers, respectively. Each dimensionless parameter is described as follows. First, Reynolds number (Re) describes the ratio between the inertial forces and viscous forces. Furthermore, the analysis also utilizes the Weber number (We), which represents the ratio between the inertial force and surface tension force. Next, Ohnesorge number (Oh), is used to explain the relationship between the viscous forces to inertial and surface tension forces. Next, it is understood that the surface temperature also plays an important role in droplet behavior. Under similar experimental condition (surface material, the distance between the droplet generator and the testing material, the droplet impact velocity, and the initial droplet diameter), the surface temperature was also varied between 110 and 240 °C, with an interval of 10 °C, to represent different boiling regime.

The behavior of the successive droplets during the impacting onto a hot solid surface was recorded by a high-speed video camera of phantom MIRO M310. The resolution of the camera and the frame speed were 1024 × 768 and 2000 fps, respectively. To improve the light condition, set of LED lamps were placed behind the hot surface. Between the light source and the hot surface, a diffusive layer was also installed to produce uniform lighting.

Table 1
The physical properties of tested liquid droplets at room temperature.

Fluids	ρ (kg/m^3)	σ (N/m)	μ (Pa s)	d (mm)	v (m/s)
Pure water (0 EG)	997	0.071	0.0008	3.15	1.1
10% ethylene glycol water solution (10 EG)	1008	0.057	0.0011	3.12	1.1
20% ethylene glycol water solution (20 EG)	1020	0.048	0.0014	3.16	1.1

Table 2
The dimensionless parameter.

Fluids	*We*	*Re*	*Oh*
Pure water (0 EG)	55.85	4457.8	0.00166
10% ethylene glycol water solution (10 EG)	67.02	3093.9	0.00264
20% ethylene glycol water solution (20 EG)	81.73	2278.9	0.00350

The brief procedures of this experimental study are explained as follows. First, the tanks storage was filled the working fluid. In this process, it was important to ensure that the tank storage and other parts of the droplet were clean in order to prevent any impurities. Then, the droplet injector was set as required by the present study. After the droplet generator was ready, the stainless steel specimen was placed on the induction heater. The calibration process of the thermocouple was done to maintain the accuracy of the measurement process. At the same time, the high-speed camera and the illumination system were also prepared. After all of the experimental apparatus was set, the induction heater was turned on, and the stainless-steel surface temperature gradually increased. As the desired temperature achieved, the droplet was released from the generator, and the behavior of the droplet was recorded by the high-speed camera. For each surface temperature, the experiments were repeated three times to ensure the similarity of the phenomena. Those steps were conducted for all of the parameters investigated in this study the variation of surface temperature and ethylene glycol concentration.

After the video images of the successive droplets were recorded, those were transferred to the personal computer to conduct a detailed analysis by image processing technique. The developed image processing technique was implemented to obtain the quantitative parameter of the droplet. The sequence steps of the implemented image processing technique are as follows. First, the raw image was loaded, and followed by cropping and rotating function to remove the unnecessary part and to fix the misalignment on the horizontal axis, as shown in Fig. 4a. Next, a median filter was applied to reduce the noise. In the present work, the quality of the raw image was already good. Hence, no more pre-processing steps were needed.

Furthermore, the images were converted into a binary image, as shown in Fig. 4b. The threshold value was determined carefully since it strongly affects the contour of the droplet. In most cases, the value of 0.50 was used as the threshold value. As the object representing the droplet was successfully determined, the interfacial can be detected by using the "find edge" function in a commercial MATLAB software. As shown in Fig. 4c, the edge of the object, as illustrated with a red line, shows a good agreement when it is overlapped with the raw image. If the results are unsatisfactory, the threshold value should be evaluated. The last is the measurement of the spreading diameter and the height of the droplet by tracking the position of the edge of the droplet, as shown in Fig. 4d. In the analysis, the measurement data were focused on the time variation of the spreading ratio and the apex height of the droplet. Here, the spreading ratio (d/d_o) is defined as the ratio of the droplet-spreading diameter (d) to the initial droplet diameter (d_o). In addition, Apex height (h/d_o) is the ratio of the droplet height (h) to the initial droplet diameter (d_o). The spreading ratio and apex height than are arranged in the form of time-series data, to ease the analysis of droplet phenomena, the dimensionless time (τ) is utilized and is defined:

$$\tau = \frac{t.v}{d_0} \tag{1}$$

where t is time measured from the first impact, v is the impact velocity, d_o is the initial impact diameter of the droplet. $\tau = 0$ is the initial time of the droplet starts to impact the hot surface.

During the experiments, it is important to reveal how the uncertainties and errors caused by the measurement data acquisition process affect parameter determination. The first component is the uncertainty produced by the sensor and data logger. The sensitivity of sensors is 0.5%, whereas the Lutron logger TM-946, used to measure and record the temperature data, has an uncertainty of 0.05% for K-type thermocouple in range −199.9 to 1370 °C.

Regarding the visual data recording, which is later processed to produce quantitative data, the errors are strongly associated with the image resolution resulted from the comparison between the dimension of certain objects with its pixel size. In the present study, the object with a length of 50 mm was recorded in 727 pixels image. Therefore, the resolution of the image is 0,069 mm/pixel. A similar approach to conducting error analysis was carried out by Mitrakusuma et al. [39] on the basis of the approach of Taylor [40]. For instance, the uncertainty of Weber number [$We = \rho v^2 D/\sigma$], in general, can be defined as follows.

$$\Delta We = \sqrt{\left(\frac{\partial We}{\partial \rho}.\Delta\rho\right)^2 + \left(\frac{\partial We}{\partial \sigma}.\Delta\sigma\right)^2 + \left(\frac{\partial We}{\partial v}.\Delta v\right)^2 + \left(\frac{\partial We}{\partial D}.\Delta D\right)^2} \tag{2}$$

The property of surface tension and density were assumed to be constant during the experiment. Then the uncertainty of Weber Number

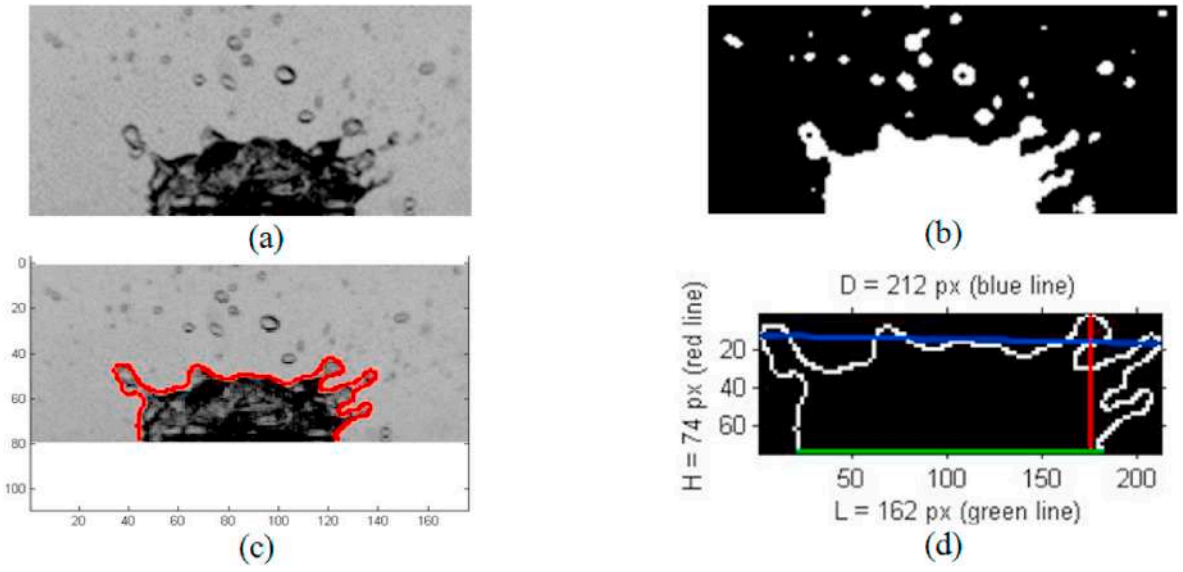

Fig. 4. The sequence steps of image processing technique used in the present work. (a) raw image, (b) binary image, (c) the object perimeter, (d) parameter measurement.

can be written as follows.

$$\Delta We = \frac{\rho}{\sigma}\sqrt{(2.v.D.\Delta v)^2 + (v^2.\Delta D)^2} \quad (3)$$

Where the Δv and ΔD represent the uncertainty of velocity and the diameter of the droplet, respectively. The summary of uncertainty analysis is shown in Table 3.

3. Result and discussions

In the next section, the collision behavior of the first droplet and the second droplet is analyzed to obtain the behavior of the successive droplets impacting onto a hot solid surface. The discussion will concentrate on the dynamic behavior of successive droplets impacting onto a hot solid surface in the region of the surface temperatures from the nucleate boiling to the critical heat flux (CHF). The effects of the additional ethylene glycol on the water solution, which directly affect the fluid properties such as the boiling temperature, viscosity, and the surface tension, are also considered.

3.1. Collision dynamics of the first and second droplets impacting

3.1.1. Surface temperature is 110 °C

Fig. 5 shows the interfacial behavior of the first droplet impacting onto a hot solid surface at the surface temperature of 110 °C to represent the bubble formation nearly the region of nucleate boiling. The tested fluids were pure water (0 EG), 10% ethylene glycol water solution (10 EG), and 20% ethylene glycol water solution (20 EG). The figure shows that the addition of ethylene glycol affects the bubble entrainment behavior. Close observation of Fig. 5 reveals that the first tiny bubble generation inside the droplet of 0 EG, 10 EG, and 20 EG occur at τ = 7.05, 8.23, and 10.19, respectively. It means that the addition of ethylene glycol postpones the onset of the boiling of the solution, whereas the tiny bubble grows slower at a higher concentration of ethylene glycol. The trapped bubble mechanism inside the impacting droplet was clearly explained by Nejad et al. [41]. They reported that under room temperature, it is generated by the presence of trapped air during the initial contact of the droplet and the surface. As the droplet hits the surface, the air below the droplet is forced out to produce a sudden increment of the pressure gradient between the droplet and the surface. It leads to the formation of the bubble entrainment, as also reported by Liang et al. [16], who investigated the contact vaporization during the droplet impinging onto a hot surface.

Fig. 6 shows the time variation of the droplet interfacial behavior during the successive droplets impacting onto a hot solid surface at the surface temperature of 110 °C. Moreover, the time variations both of d/d_o and h/d_o are shown in Fig. 7. From the visual observation, it is noticed that in general, the droplet interfacial behaviors of 0 EG, 10 EG, and 20 EG are similar during the impact process. In Fig. 6, $\tau = 0$ represents the initial impact time of the droplet. As soon as the first droplet impacts the hot surface, the droplet spreads to form a disk shape liquid. It is due to the sudden change of the momentum from vertical to the radial direction. The droplet then expands to the maximum diameter. On the other hand, as shown in the upper part of Fig. 7, the h/d_o decreases gradually during the spreading process and reaches the minimum value. The maximum d/d_o is achieved around τ = 2.35 and characterized by the occurrence of a flat liquid surface surrounded by the thicker liquid film. The maximum d/d_o of 0 EG, 10 EG, and 20 EG are achieved at 2.52, 2.59, and 2.66, respectively. Next, the addition of 20% ethylene glycol on the water solutions gives the highest of the maximum d/d_o of the first droplet. It is caused by the presence of ethylene glycol, which decreases the surface tension of the liquid droplet. Therefore, the droplet spreads more easily at a higher concentration of ethylene glycol.

Further observation of Figs. 6 and 7 indicate that as time goes by, the droplet interfaces move back to the center, and the recoil process occurs at τ = 3.52. The d/d_o decreases until below 2, and the droplet keeps their position to stick on the hot surfaces. The obtained results are in good agreement with Bai and Gossman [42], who developed a methodology for spray impingement simulation for the automotive simulation applications. Next, as also shown in Fig. 7, the h/d_o of 0 EG droplet increases gradually, whereas the d/d_o drops significantly. On the other hand, the changes of the d/d_o and the h/d_o of 10 EG and 20 EG droplets are not as high as of 0 EG. It is due to the change of the liquid viscosity influenced by the addition of ethylene glycol. In detail, the lower the concentration of ethylene glycol concentration, the lower the viscosity of the liquid. Here, the viscosity acts as a resistive force to dissipate the flow induced by the capillarity force. As a result, the droplet does not show a significant recoiling process. In addition, 0 EG contains relatively low viscosity and high surface tension. The potential energy resulted from the impact processes is partially converted into kinetic energy. Consequently, the droplets recoil faster, and a high deviation during recoil and the oscillation process can be observed. The observed phenomena are also in good agreement with that of Kim and Chun [43]. After the droplet reaches the maximum recoiling process, the droplet oscillates several times until it reaches a stable condition. The droplet oscillation occurs due to the difference in the momentum and pressure between the droplet and its surroundings, as also reported by Mitrakusuma et al. [39].

In the next section, the phenomena around the impingement of the second droplet will be discussed. Since the surface temperature is still low, the first droplet tends to stay on the surface. Next, the second droplet hits precisely the center of the first droplet. After the first droplet coalesces with the second droplet, the liquid swelling of the coalescence droplet occurs. The liquid swelling is caused by force from the impact velocity of the second droplet, as reported also by Fujimoto et al. [44]. It results in the radially spreading on the upper part of the first droplet, which increases the d/d_o. As shown in Fig. 7, the maximum d/d_o increases significantly due to the presence of the second droplet. The figure also shows that the maximum d/d_o of the 0 EG, 10 EG, and 20 EG are 3.04, 3.10, and 3.26, respectively. It is also noticed that the presence of the second droplet also causes the coalescence droplet stays at a longer time on a hot solid surface. Therefore, it increases the amount of heat transferred from the hot surface to the liquid.

3.1.2. Surface temperature is 160 °C

It should be noted from the previous investigations that the increase of surface temperature affects the droplet impact behavior. Here, the surface temperature was set at 160 °C, representing the phenomena around the transition boiling region. It is also essential to investigate whether the change of fluid properties affects the droplet dynamics. Fig. 8 shows the dynamics behavior of 0 EG, 10 EG, and 20 EG during the successive droplets impacting onto a hot solid surface of the surface temperature of 160 °C, while Fig. 9 shows the evolution of the corresponding both of d/d_o and h/d_o. As shown in Fig. 8, after the first droplet impacts the hot surface, the generation of the tiny bubbles due to the boiling process can be easily observed at the droplet surface. Close

Table 3
The uncertainty of *We*.

Fluid of droplet	The height of syringe, h (m)	Δh (m)	Droplet diameter, D (m)	ΔD (m)	Droplet velocity, V (m/s)	ΔV (m/s)	*We*	Δ*We*
0 EG	0.050	0.001	0.00315	0.000069	1.1	0.0035	55.85	1.24
10 EG	0.050	0.001	0.00312	0.000069	1.1	0.0035	67.02	1.48
20 EG	0.050	0.001	0.00316	0.000069	1.1	0.0035	81.73	1.54

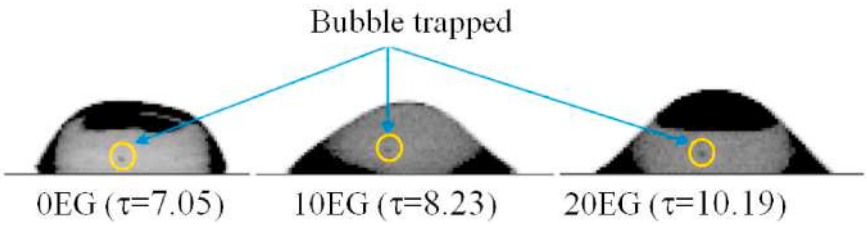

Fig. 5. Rise bubble entrainment at temperature 110 °C.

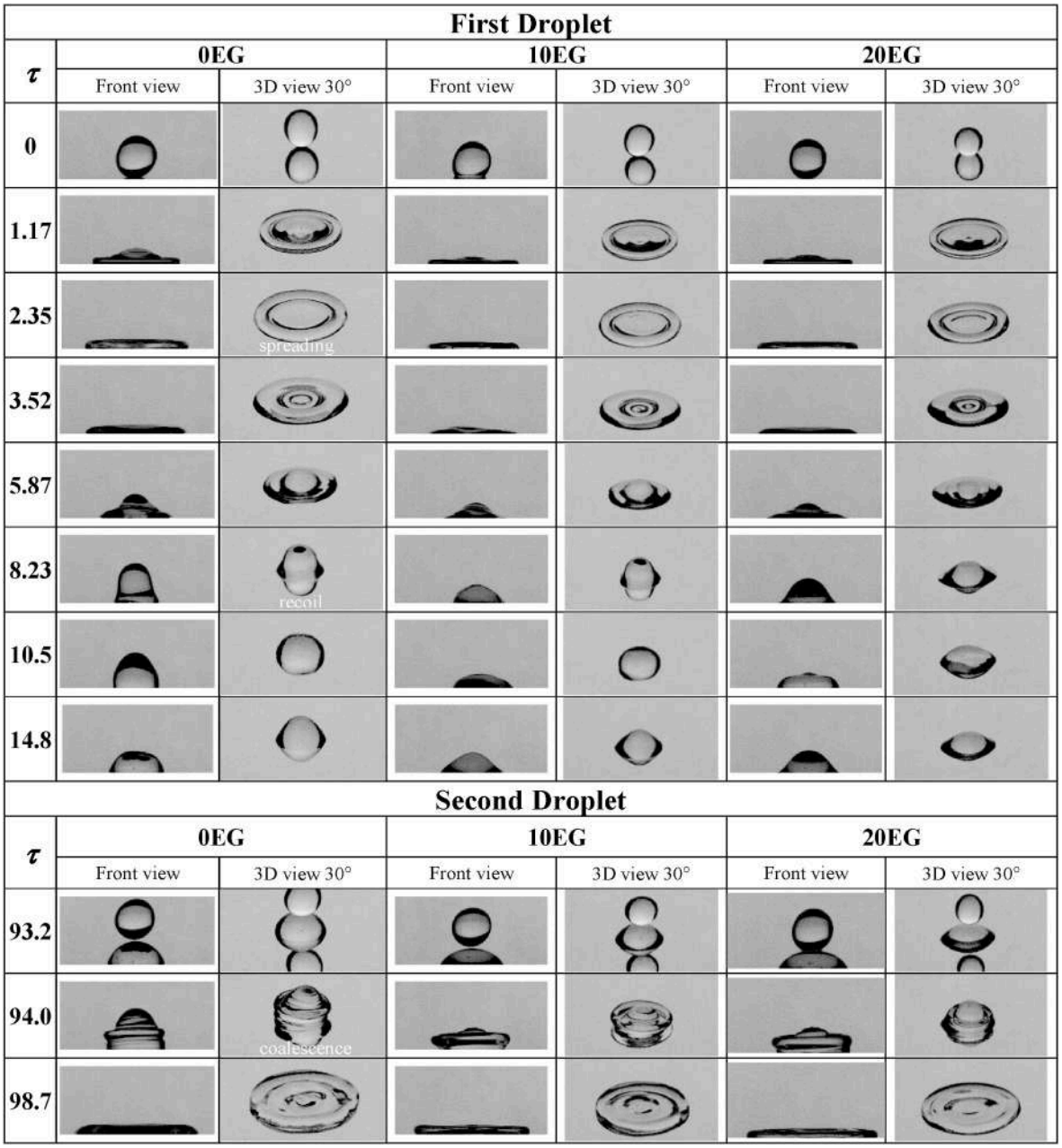

Fig. 6. The sequence images of the successive multiple droplets impacting the hot surface of 0 EG, 10 EG, and 20 EG at temperature 110 °C.

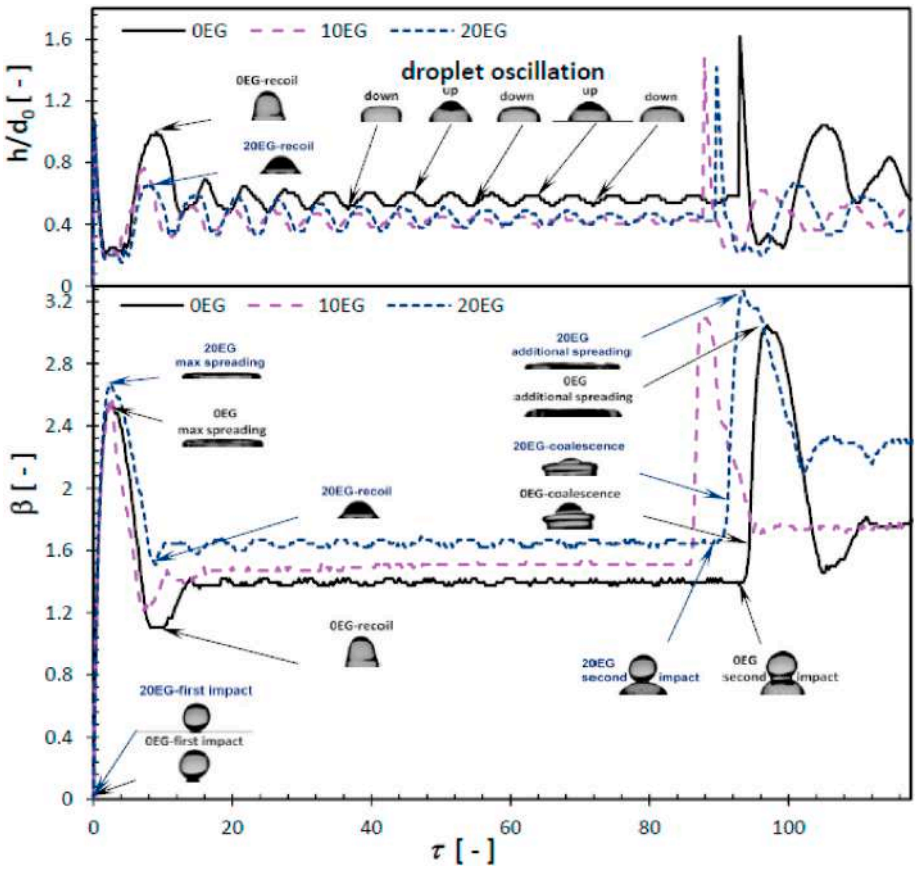

Fig. 7. The evolution of spreading ratio and apex of successive multiple droplets 0 EG, 10 EG, and 20 EG at temperature 110 °C.

observation of the figure reveals that there are more generated tiny bubbles on the 0 EG droplet compared to that of both of 10 EG and 20 EG. This means that the boiling exists earlier at a lower concentration of ethylene glycol.

In terms of the spreading phenomenon, it is found that the 20 EG produces the highest $d/d_{o,}$ as shown clearly in Fig. 9. The maximum d/d_o of 20 EG, 10 EG, and 0 EG are 2.95, 2.62, and 2.68, respectively. The detail observation on the recoil process indicates that the 0 EG droplet produces the highest h/d_o. It can be explained as follows. The transferred heat from the hot surface to the liquid causes the presence of a local temperature difference inside the droplet. The natural convection leads the liquid motion and creates a local fluid flow. However, the obtained energy from the droplet impact is big enough to overcome the local turbulence inside the liquid. Therefore, the droplet behavior is the same as the surface temperature of 110 °C. As time progresses, a number of the tiny bubbles were formed. It is due to a higher heat transfer rate from the hot surface to the droplet, as reported by Riswanda et al. [45]. The number of transferred heats from the hot surface to the liquid also rises, which leads to the increase of the number of tiny bubbles inside the liquid droplet. The boiling point of the 0 EG droplet is achieved faster than that of 10 EG and 20 EG, hence the number of tiny bubbles in 0 EG increases significantly. Here, the small bubble interaction and the liquid flow turbulence inside the liquid droplet lead the droplet to expand. As a result, the d/d_o of the 0 EG droplet during the recoil process is slightly higher than that of 10 EG and 20 EG. The presence of the small bubble inside of the liquid also influences the surface of the droplet. The higher amount of the small bubble causes the droplet surface is not as smooth as that of 10 EG and 20 EG, in which the droplet tends to be wavy.

As time progresses to $\tau = 66.6$ as shown in Fig. 8, it is observed that the evolution of d/d_o and h/d_o are strongly influenced by the behavior of the generated bubble inside the liquid. The obtained phenomenon is quite different from that of the previous case at the surface temperature of 110 °C, where the momentum of the droplet plays an important role. As shown in Fig. 9, the second droplet hits the first droplet at around $\tau = 90.9$. Quantitatively, the presence of the second droplet improves the $d/d_{o,}$ which represents the wettability of the droplet. Moreover, it is also observed that after the droplet coalescence, the fluctuation on the droplet surface suddenly decreases. At $\tau = 94.0$, the droplet surface looks smoother, and the center of droplet almost free from the small bubble, as shown clearly in Fig. 8.

Fig. 10 shows the detailed illustration of the droplet expansion due to the presence of a generated bubble inside the droplet. The expansion spreading droplet is affected by the boiling point of the droplet. Generated bubble inside the droplet causes both of $d/d_{o,}$ and h/d_o tend to increase during the time. In addition, the formation of the secondary droplet was also detected during this phase. Cossali et al. [46] noted that the presence of secondary droplets is strongly related to the bubble behavior inside the liquid droplet. As the droplet impacts onto a hot solid surface, the heat is transferred from the surface into the liquid. The boiling triggers the formation of the small bubbles. The bubble grows and breaks the liquid lamella to form a secondary droplet. Another important thing should be considered that the secondary droplet is firstly observed at the 0 EG droplet ($\tau = 5.48$) while it appears at 10 EG and 20 EG at $\tau = 6.66$ and 10.97, respectively. The possible reason is at a lower liquid viscosity, and the droplet tends to separate easily to form the tiny satellite droplets, as also reported by Bernardin et al. [2].

3.1.3. *Surface temperature is 210 °C*

Fig. 11 shows the dynamics of the first and second droplets impacting onto a hot solid surface of 0 EG, 10 EG, and 20 EG at the surface temperature of 210 °C, in which the corresponding evolution of d/d_o and h/d_o are depicted in Fig. 12. This surface temperature represents the temperature in the region of transition boiling. As shown in Fig. 11, the observed phenomena are almost the same as the phenomena the surface

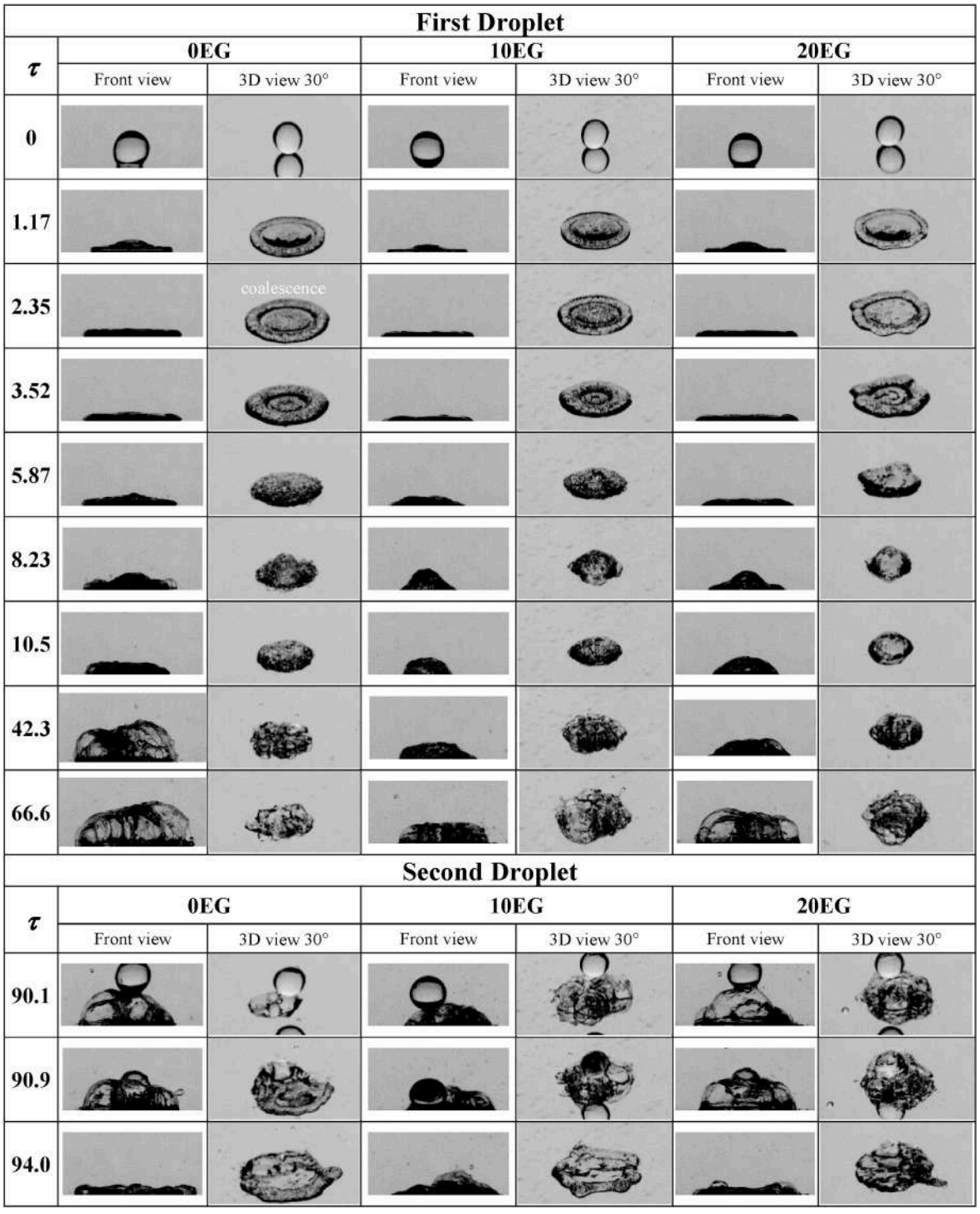

Fig. 8. The sequence of images of the successive multiple droplets impact process of 0 EG, 10 EG, and 20 EG at temperature 160 °C.

temperature of 160 °C. That is, the generated bubbles increase more easily at 0 EG than that of 10 EG and 20 EG. Next, the droplet surface becomes lumpier for all the tested liquids. Those are shown clearly at $\tau = 2.35$. On the other hand, it is also noticed that the maximum d/d_o of 0 EG is achieved at $\tau = 3.13$ while that of both of 10 EG and 20 EG are at $\tau = 2.35$. As the heat transfer process from the surface to the liquid occurs, the presence of local liquid flow and a high number of generated tiny bubbles causes the spreading process at 0 EG is slightly interrupted.

Next, the droplet starts to recoil as soon as the maximum spreading diameter is achieved. This process is followed by the boiling process on the droplet body. The maximum h/d_o of 0 EG, 10 EG, and 20 EG droplets are 1.36, 0.96, and 1.13, respectively, as depicted clearly in Fig. 13. The figure shows that more secondary droplets, both vertical and horizontal directions, were observed in comparison to that the lower surface temperature. At 0 EG, the boiling occurs faster and leads to the formation of a thin vapor layer below the droplet. Due to the 0 EG, the droplet has the lowest boiling point. Therefore, the droplet recoil and the maximum h/d_o occurs easily.

After the recoil of the 0 EG, the d/d_o decreases, while the d/d_o both of 10 EG and 20 EG tend to increase slightly. Close observation of Fig. 12

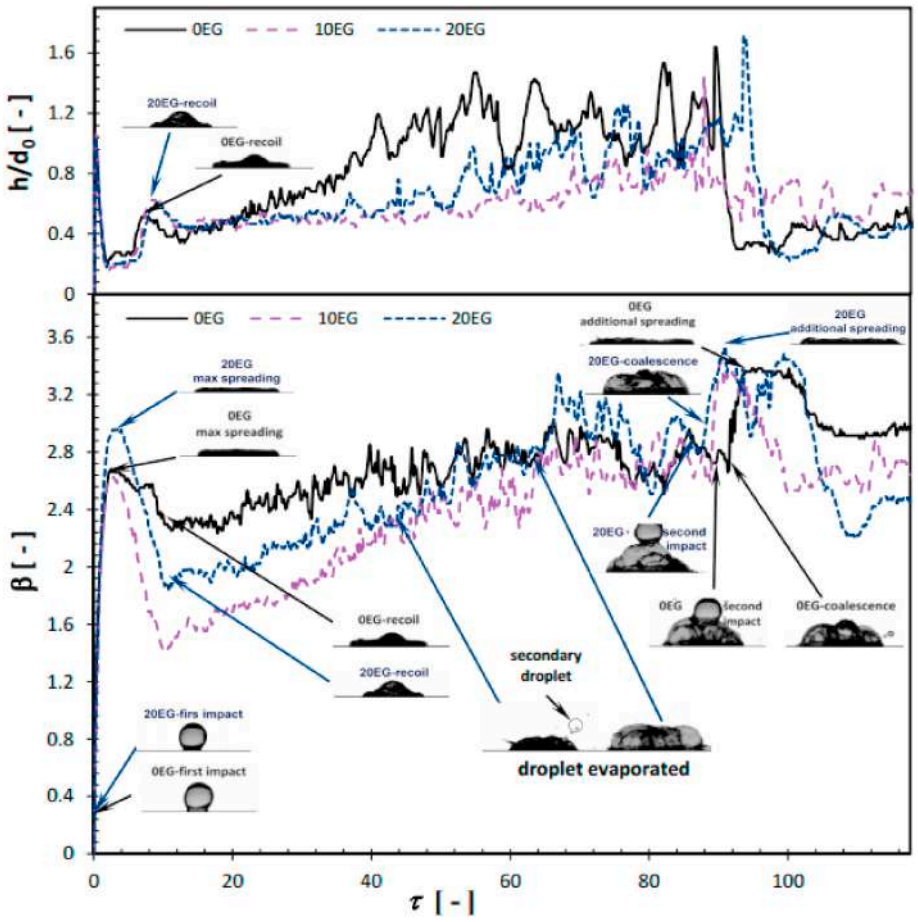

Fig. 9. The evolution of spreading ratio and apex of successive multiple droplets 0 EG, 10 EG, and 20 EG at temperature 160 °C.

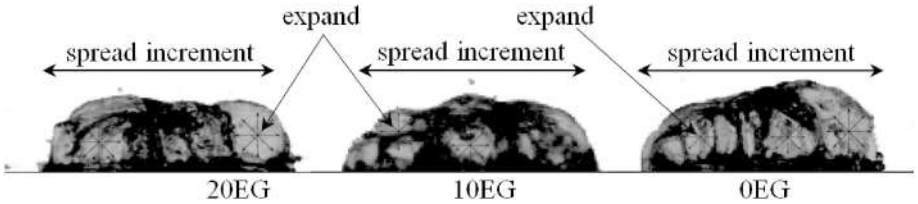

Fig. 10. Droplet spread increasing due to the expansion of bubble entrainment at the bubble inside the droplet at temperature 160 °C.

reveals that at 0 EG, the occurrence of the secondary droplet is more often observed in comparison to that of 10 EG and 20 EG. As a result, the droplet volume of 0 EG reduces significantly, and the d/d_o decreases. Although the volume of 0 EG loses partially due to the formation of the secondary droplet, the droplet is still able to stick on the hot surface until the presence of the second droplet. From the visual observation, it can be concluded that the presence of the second droplet has successfully improved the wettability. Similar to the previous cases, the 20 EG droplet shows the highest maximum d/d_o. In detail, the maximum d/d_o for 0 EG, 10 EG, and 20 EG are 3.02, 3.12, and 3.78, respectively.

The analysis of the observed phenomena indicates that at the surface temperature of 110 °C, the droplet tends to be stable after the second droplet impacts. While at the surface temperature of 160 °C, the expansion process due to the bubble growth and fluid turbulence causes the increase of d/d_o. At a higher surface temperature of 210 °C as an example, the d/d_o generally decreases due to a higher rate of the evaporation and the formation of the secondary droplets.

3.2. Effect of the second droplet impact on the collision behavior

The increase of d/d_o during the successive droplets phenomena are strongly affected by the condition of the first droplet before the appearance of the second droplet, whether it spreads, recoils, bounces, or splashes. Fig. 14 shows the obtained phenomena during the impact of the second droplet under the various surface temperatures. Here, the 20 EG is taken as an example. Close investigation on the figure reveals that at the surface temperature of 110 °C, the second droplet appears when the first droplet spreads and completely sticks with hot surfaces. As a result, the second droplet effectively coalesces. Therefore, the d/d_o can be improved. While at the surface temperature of 160 °C, the first droplet boiled and followed by the expansion process. The secondary droplet starts to appear and results in a decrease in droplet volume. The presence of the second droplet successfully improves the d/d_o, although it is not as effective as the case of the surface temperature of 110 °C. At the surface temperature of 210 °C, the evaporation rate increases, and more secondary droplets were generated. Therefore, the droplet volume decreases significantly. At this surface temperature, the increase of d/d_o

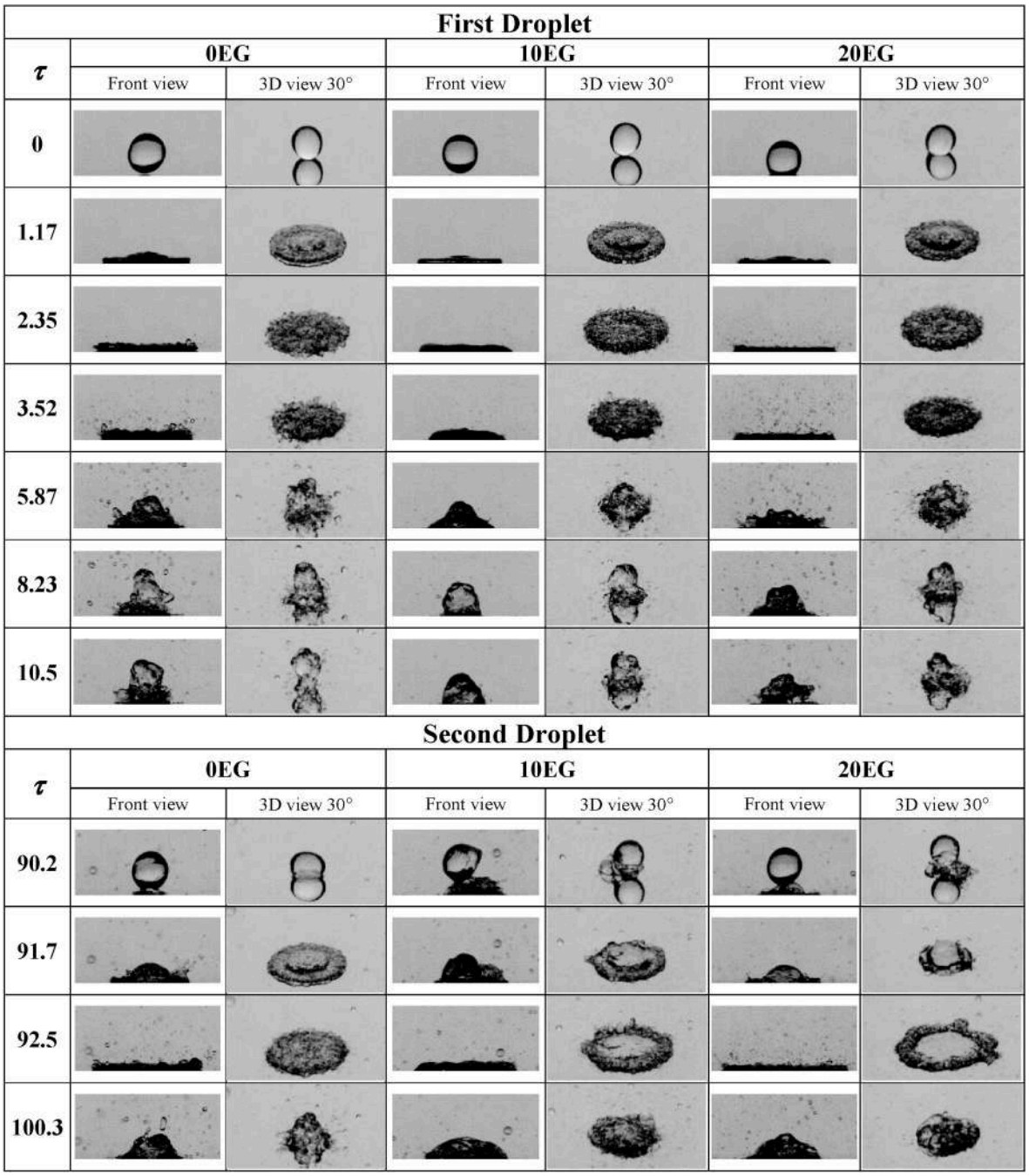

Fig. 11. The sequence of the images of the successive multiple droplets impact onto the hot solid surface of 210 °C.

due to the presence of the second droplet is smaller than that of 110 °C and 160 °C.

Fig. 15 shows the visualization of the droplet impingement onto a hot solid surface at the surface temperature of 230 °C. Fig. 15 (a), (b), and (c) correspond to the cases of 0 EG, 10 EG, and 20 EG, respectively. The research on the droplet interaction, such as conducted by Piskunov et al. [22] and Kuznetsov et al. [35], points out the importance of investigating this phenomenon, which strongly affected by component concentrations and fluid properties. In Fig. 15(a), the first droplet bounces and moves from the initial impact position. While Fig. 15(b) shows that the first droplet of the 10 EG maintains its position, so the second droplet can significantly improve the d/d_o since it completely hits the first droplet. During the impact phenomena of 10 EG, the first droplet tends to stay in the initial position because of the slower rate of the boiling process. In addition, the droplet only experiences a small change of the surface tension, the impact phenomena of the 20 EG depicted in Fig. 15 (c). Here, the 20 EG droplet shows similar behavior to that of 10 EG, whereas the first droplet tends to maintain its initial position. Both phenomena can be classified into the regime of coalescence in which the droplets merge into a single droplet and support the cooling process, as suggested by Piskunov et al. [22]. Although the evaporation rate in the high temperature leads to the presence of a gas-vapor layer around the droplet, the kinetic energy of the second droplet is able to overcome the layer. Therefore the coalescence process occurred. Equally important, this finding reveals the effect of ethylene glycol addition on droplet behavior, in which the addition increases the boiling point of the mixtures. Furthermore, it delays the formation of the thin gas film under the droplet. Hence, it is able to hold its position until the impact of the

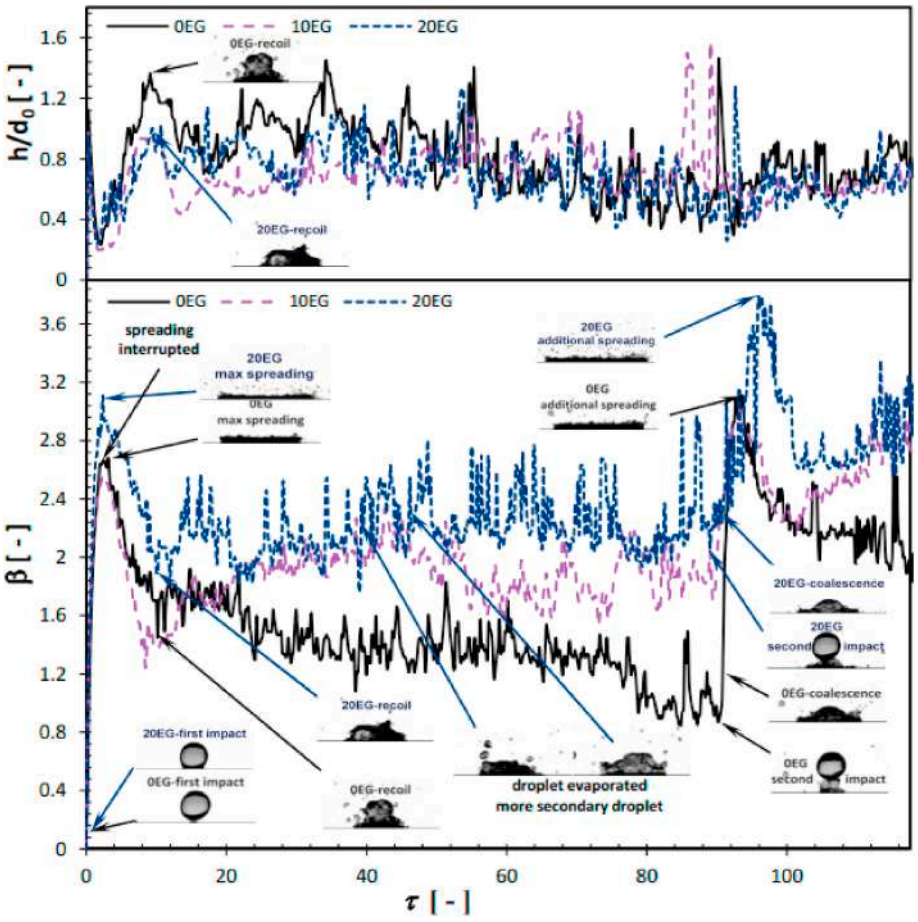

Fig. 12. The evolution of the spreading ratio and the apex height of successive multiple droplets of 0 EG, 10 EG, and 20 EG at the surface temperature 210 °C.

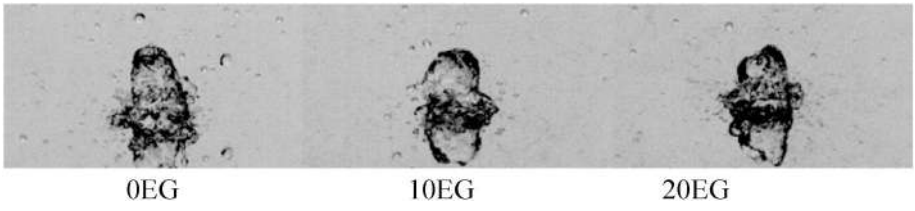

Fig. 13. Visualization of the apex maximum droplets at 210 °C.

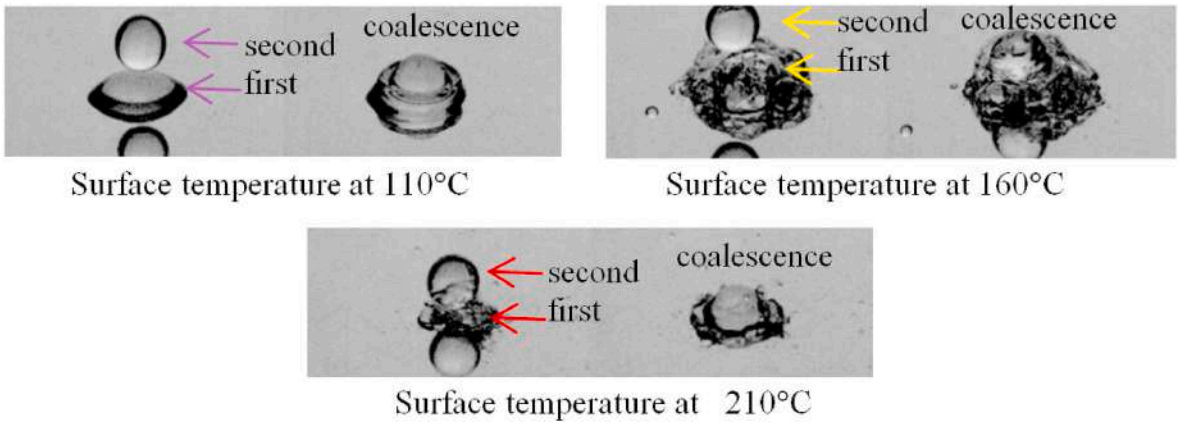

Fig. 14. The Visualization of the coalescence of the droplets at 20 EG droplet.

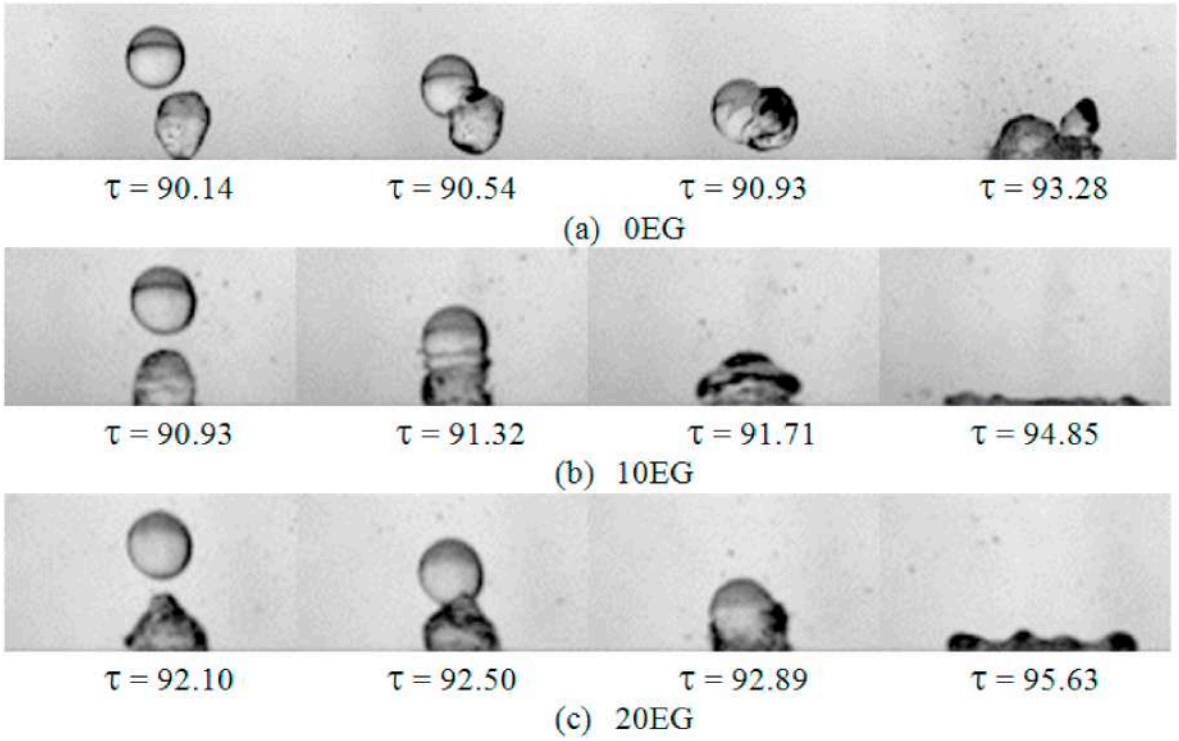

Fig. 15. Visualization of the droplets coalescence at the surface temperature 230 °C.

second droplet.

3.3. Maximum spreading ratio

Fig. 16 shows the effect of the surface temperatures and ethylene glycol concentration on the maximum d/d_o obtained from the present work. As shown in the figure, in the range of the surface temperatures of 110 °C–120 °C, the maximum d/d_o is affected by the dynamics of the impacting of the first and second droplets. On the other hand, in the temperature range of 130 °C–230 °C, the first droplet experience various phenomena, such as the evaporation, the bubble generation, and the presence of secondary droplets. It causes the fluctuation of the maximum d/d_o. If the surface temperature is increased higher than 240 °C, the thin vapor layer below the first droplet leads the bouncing of the first droplet from the hot surface. Consequently, the maximum d/d_o after the presence of the second droplet does not increase significantly.

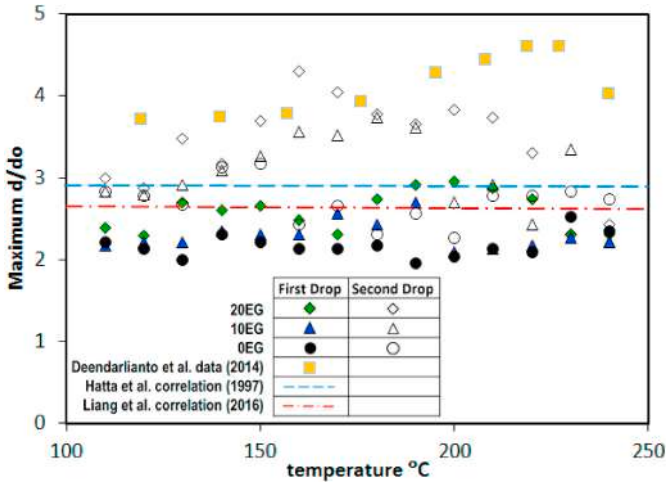

Fig. 16. Spreading ratio maximum at first droplet and the second droplet.

Next, the comparison of the maximum spreading ratio obtained from the present work and available correlation from the previous researches, as indicated in Table 4, is depicted in Fig. 16. The figure also consists of the data of Deendarlianto [1], who investigated the behavior of droplets impacting two modules of stainless steel coated by TiO_2. The figure reveals that the behavior of the first droplet impacts strongly affecting by Weber number as suggested by Liang et al. [47] and Hatta et al. [48]. From those facts, it can be noticed that the available correlations were formulated only based on the first droplet impact phenomena. As shown in the figure, the correlation from Liang et al. [47] and Hatta et al. [48]. Overpredict to the present experimental data. The possible reason for the discrepancy is that the available correlations were developed under different experimental conditions such as solid surface material and liquid properties. Furthermore, the present data underestimate to that of Deendarlianto et al. [1] who conducted the experimental study under a higher impact velocity. The above facts indicate that the maximum spreading velocity of a droplet impacting a hot solid surface is strongly affected by the experimental conditions and the liquid properties. Hence, it is important to conduct a further experimental study to obtain high-quality data to formulate a new correlation, which represents the physics of successive droplets impacting onto a hot solid surface.

The Weber number becomes one of the most important parameters to explain the change of droplet behavior associated with initial force and surface tension force [11]. As mentioned in Table 2, it is understood that the addition of ethylene glycol, triggering the change of several fluid properties, directly affects the Weber number. In detail, the Weber

Table 4
The correlations of maximum spreading diameter obtained from previous studies.

Author	Fluid (s)/Wall material (s)	Experimental Correlation
Liang et al. [47]	Water, ethanol and butanol, polished stainless steel	$D^*_{max} = 0.788We^{0.306}$
Hatta et al. [48]	Water, Inconel 625, stainless steel	$D^*_{max} = 0.093\ We^{0.74} + 1$

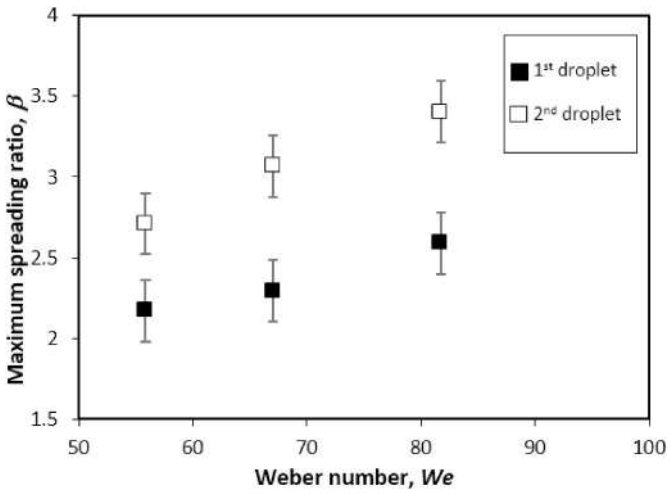

Fig. 17. The relationship between the Weber number and the maximum spreading diameter of both first and second droplets during the impacting of multiple droplet onto a hot solid surface.

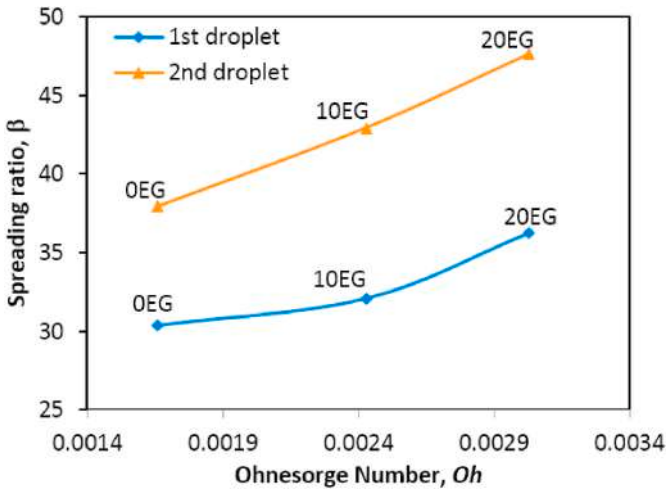

Fig. 18. The effect of Ohnesorge number on the cumulative maximum spreading ratio after the presence of the first droplet and second droplet.

numbers of 0 EG, 10 EG, and 20 EG solution are 55.85, 67.02, and 81.73, respectively. Fig. 17 depicts the effect of Weber number on the maximum spreading ratio of the droplet. In general, it consists of the data on the condition after the first and second droplet impact. Each point represents the average of data gathered from a surface temperature between 110 °C and 240 °C, with an interval of 10 °C. The figure shows that the maximum spreading ratio, both after the first and second droplet impact, rise as the increase of Weber number. For instance, on the phenomenon after the impact of the second droplet, the maximum spreading ratio at Weber number of 55.85 is 2.17. The maximum spreading ratio increases to 2.29 at Wb number of 67.02 and becomes larger, around 2.58, at the Weber number of 81.73.

Further analysis should be conducted to support the findings related to droplet behavior. While the Weber number has successfully described the dynamics of the droplet during the impact, in-depth analysis covering the effect of those fluid properties should be elaborated by utilizing the Ohnesorge number as suggested by Chen et al. [49]. Ohnesorge number, as indicated in Table 2 for all of the working fluid, is strongly related to the resistive force during the spreading process. Fig. 18 shows that the increase of Ohnesorge number is also followed by an increase in the maximum spreading ratio. Close observation of the figure reveals that the ratio of the increase of Ohnesorge number is slightly higher than that of the ratio of increase of the spreading ratio. This means that the effect of viscosity is more dominant than that of surface tension during the impacting of successive droplets onto a horizontal hot solid surface. The figure shows that the increase of the maximum d/do due to the addition of 10%, and 20% ethylene glycol on the pure water solution is obtained around 6.2% and 19.3%, respectively. In addition, the increase of maximum d/do due to the presence of the second droplet on the 0 EG, 10 EG, and 20 EG droplets are 24.8%, 33.3%, and 31.4%, respectively. Therefore, it can be concluded that the increase of the concentration of ethylene glycol, which directly reduces the surface tension, increases the spreading ratio.

4. Conclusions

The visualization study of the effect of the concentration of ethylene glycol on the interfacial dynamics of the successive droplets impacting onto a horizontal hot solid surface was carried out. The concentration of ethylene glycol on the solution was varied from 0 to 20%. The results are summarized as follows:

1. Ethylene glycol plays a significant role in the dynamic behavior of the successive droplets impacting onto a horizontal hot solid surface. At the surface temperature of 110 °C, the increase of the concentration of ethylene glycol causes the decrease of the droplet oscillation after the spreading phase. In addition, the postpone growth of tiny bubbles was also detected due to the addition of the concentration of ethylene glycol.
2. The addition of the concentration of ethylene glycol decreases the spreading velocity. It is strongly affected by the presence of resistant forces, which increases as the increase of the liquid viscosity. Next, the formation of the secondary droplet is delayed with the increase of the concentration of ethylene glycol.
3. The presence of the second droplet, in general, improves the wetting area of the droplet. The droplet at the surface temperature of 110 °C sticks with the hot surfaces during the presence of the second droplet, which leads to the effective coalescence phenomenon. While at the temperature of 160 °C and 210 °C, the first droplet has experienced the volume decrease due to secondary droplets.
4. The Weber number plays an important role on the maximum spreading diameter during the impacting of multiple droplets onto a hot solid surface, in which the higher the Weber number, the higher the maximum spreading droplet diameter of both first and second droplets.
5. Addition of ethylene glycol causes the increase of the maximum d/d_o. The increase of the maximum d/d_o due to the addition of 10% and 20% ethylene glycol on the pure water solution is obtained around 6.2% and 19.3%, respectively. Furthermore, the presence of the second droplet improves the wettability of the droplet. The increase of maximum d/d_o due to the presence of the second droplet on the 0 EG, 10 EG, and 20 EG droplets are 24.8%, 33.3%, and 31.4%, respectively.

Declaration of competing interest

The authors declare that they have no known competing financial interests or personal relationships that could have appeared to influence the work reported in this paper.

Acknowledgements

The work was carried out within a special research project funded by Gadjah Mada University under the scheme of “Rekognisi Tugas Akhir”. The project number is 2127/UN1/DITLIT/DIT-LIT/LT/2019. The authors also would like to express their sincere appreciation to the member

of the Fluid Mechanics Laboratory, Department of Mechanical and Industrial Engineering, Faculty of Engineering Gadjah Mada University, for their support.

Appendix A. Supplementary data

Supplementary data to this article can be found online at https://doi.org/10.1016/j.ijthermalsci.2020.106594.

References

[1] Deendarlianto, Y. Takata, S. Hidaka, Indarto, A. Widyaparaga, S. Kamal, Purnomo, M. Kohno, Effect of static contact angle on the droplet dynamics during the evaporation of a water droplet on the hot walls, Int. J. Heat Mass Tran. 71 (2014) 691–705, https://doi.org/10.1016/j.ijheatmasstransfer.2013.12.066.

[2] J.D. Bernardin, C.J. Stebbins, I. Mudawar, Mapping of impact and heat transfer regimes of water drops impinging on a polished surface, Int. J. Heat Mass Tran. 40 (1997) 247–267, https://doi.org/10.1016/0017-9310(96)00119-6.

[3] S.L. Manzello, J.C. Yang, An experimental investigation of water droplet impingement on a heated wax surface, Int. J. Heat Mass Tran. 47 (2004) 1701–1709, https://doi.org/10.1016/j.ijheatmasstransfer.2003.10.020.

[4] J. Shen, C. Graber, J. Liburdy, D. Pence, V. Narayanan, Simultaneous droplet impingement dynamics and heat transfer on nano-structured surfaces, Exp. Therm. Fluid Sci. 34 (2010) 496–503, https://doi.org/10.1016/j.expthermflusci.2009.02.003.

[5] A.S. Moita, A.L.N. Moreira, Drop impacts onto cold and heated rigid surfaces: morphological comparisons, disintegration limits and secondary atomization, Int. J. Heat Fluid Flow 28 (2007) 735–752, https://doi.org/10.1016/j.ijheatfluidflow.2006.10.004.

[6] A.K. Thokchom, Q. Zhou, D. Kim, D. Ha, T. Kim, Characterizing self-assembly and deposition behavior of nanoparticles in, Sensor. Actuator. B Chem. (2017), https://doi.org/10.1016/j.snb.2017.06.045.

[7] M. Eslamian, Spray-on thin film PV solar cells: advances, potentials and challenges, Coatings 4 (2014) 60–84, https://doi.org/10.3390/coatings4010060.

[8] M.D. King, J.C. Yang, W.C. Chien, W.L. Grosshandler, Evaporation of a small water droplet containing an additive, in: Proc. 32nd ASME Natl. Heat Transf. Conf., 1997.

[9] Q. Cui, S. Chandra, S. McCahan, The effect of dissolving salts in water sprays used for quenching a hot surface: Part 1 - boiling of singled droplets, J. Heat Tran. 125 (2003) 326–332, https://doi.org/10.1115/1.1532010.

[10] S.L. Manzello, J.C. Yang, On the collision dynamics of a water droplet containing an additive on a heated solid surface, Proc. Roy. Soc. A Math. Phys. Eng. Sci. 458 (2002) 2417–2444, https://doi.org/10.1098/rspa.2002.0980.

[11] Š. Šikalo, E.N. Ganić, Phenomena of droplet-surface interactions, Exp. Therm. Fluid Sci. 31 (2006) 97–110, https://doi.org/10.1016/j.expthermflusci.2006.03.028.

[12] Deendarlianto, Y. Takata, A. Widyatama, A.I. Majid, A. Wiranata, A. Widyaparaga, M. Kohno, S. Hidaka, Indarto, The interfacial dynamics of the micrometric droplet diameters during the impacting onto inclined hot surfaces, Int. J. Heat Mass Tran. 126 (2018) 39–51, https://doi.org/10.1016/j.ijheatmasstransfer.2018.05.023.

[13] S. Chandra, C.T. Avedisian, On the collision of a droplet with a solid surface, Proc. Roy. Soc. A Math. Phys. Eng. Sci. 432 (1991) 13–41, https://doi.org/10.1098/rspa.1991.0002.

[14] G. Liang, I. Mudawar, Review of drop impact on heated walls, Int. J. Heat Mass Tran. 106 (2017) 103–126, https://doi.org/10.1016/j.ijheatmasstransfer.2016.10.031.

[15] Y.S. Ko, S.H. Chung, An experiment on the breakup of impinging droplets on a hot surface, Exp. Fluid 21 (1996), https://doi.org/10.1007/BF00193915.

[16] G. Liang, X. Mu, Y. Guo, S. Shen, S. Quan, J. Zhang, Contact vaporization of an impacting drop on heated surfaces, Exp. Therm. Fluid Sci. 74 (2016) 73–80, https://doi.org/10.1016/j.expthermflusci.2015.11.027.

[17] N. Laan, K.G. De Bruin, D. Bartolo, C. Josserand, D. Bonn, Maximum diameter of impacting liquid droplets, Phys. Rev. Appl. 2 (2014) 1–7, https://doi.org/10.1103/PhysRevApplied.2.044018.

[18] S.G. Whisenant, L.F. Bouse, R.A. Crane, R.W. Bovey, Droplet Size and Spray Volume Effects on Honey Mesquite Mortality with Clopyralid, vol. 46, 2015, pp. 257–261, https://doi.org/10.2307/4002618.

[19] D.R. Shaw, W.H. Morris, E.P. Webster, D.B. Smith, Effects of spray volume and droplet size on herbicide deposition and common cocklebur (Xanthium strumarium) Control, Weed Technol. 14 (2000) 321–326, https://doi.org/10.1614/0890-037X(2000)014[0321:EOSVAD]2.0.CO;2.

[20] X. Zhang, O. Basaran, Dynamic surface tension effects in impact of a drop with a solid surface, J. Colloid Interface Sci. 187 (1997) 166–178, https://doi.org/10.1006/jcis.1996.4668.

[21] T. Wibowo, A. Widyatama, S. Kamal, Indarto, Deendarlianto, The dynamics behavior of successive multiple droplets impacting onto hot surface under high concentration of ethylene glycol aquades solution, AIP Conf. Proc. (2018) 30009, https://doi.org/10.1063/1.5049981.

[22] M.V. Piskunov, N.E. Shlegel, P.A. Strizhak, R.S. Volkov, Experimental research into collisions of homogeneous and multi-component liquid droplets, Chem. Eng. Res. Des. 150 (2019) 84–98, https://doi.org/10.1016/j.cherd.2019.07.030.

[23] C. Tang, M. Qin, X. Weng, X. Zhang, P. Zhang, J. Li, Z. Huang, Dynamics of droplet impact on solid surface with different roughness, Int. J. Multiphas. Flow 96 (2017) 56–69, https://doi.org/10.1016/j.ijmultiphaseflow.2017.07.002.

[24] Y. Takata, M. Kohno, S. Hidaka, T. Wakui, The effects of the surface roughness on the dynamic behavior of the successive micrometric droplets impacting onto inclined hot surfaces, Int. J. Heat Mass Tran. 101 (2016) 1217–1226, https://doi.org/10.1016/j.ijheatmasstransfer.2016.05.132.

[25] M.L. Hakim, T. Wibowo, A. Widyatama, Deendarlianto, Indarto, The effect of surface roughness on dynamic behaviour of the successive multiple droplets impacting onto aluminium hot surfaces, IOP Conf. Ser. Mater. Sci. Eng. 434 (2018), https://doi.org/10.1088/1757-899X/434/1/012183.

[26] T. Wibowo, A. Widyatama, S. Kamal, Indarto, Deendarlianto, The effects of the material conductivity on the dynamics behavior of the multiple droplets impacting onto hot surface, AIP Conf. Proc. (2018), 20015, https://doi.org/10.1063/1.5046211.

[27] E.R. Negeed, M. Albeirutty, Y. Takata, Dynamic behavior of micrometric single water droplets impacting onto heated surfaces with TiO2 hydrophilic coating, Int. J. Therm. Sci. 79 (2014) 1–17, https://doi.org/10.1016/j.ijthermalsci.2013.12.011.

[28] H. Fujimoto, S. Yoshimoto, K. Takahashi, T. Hama, H. Takuda, Deformation behavior of two droplets successively impinging obliquely on hot solid surface, Exp. Therm. Fluid Sci. 81 (2017) 136–146, https://doi.org/10.1016/j.expthermflusci.2016.10.009.

[29] T. Zhang, J.P. Muthusamy, J. Alvarado, A. Kanjirakat, Reza Sadr, Experimental and numerical visualization of droplet-induced crown splashing dynamics, J. Heat Tran. 139 (2017), 935799, https://doi.org/10.1115/1.4035579.

[30] J.P. Muthusamy, T. Zhang, J. Alvarado, A. Kanjirakat, Effects of High Frequency Droplet Train Impingement on Crown Propagation Dynamics and Heat Transfer, vol. 138, 2016, pp. 1–2, https://doi.org/10.1115/1.4032231.

[31] H. Fujimoto, Y. Oku, T. Ogihara, H. Takuda, Hydrodynamics and boiling phenomena of water droplets impinging on hot solid, Int. J. Multiphas. Flow 36 (2010) 620–642, https://doi.org/10.1016/j.ijmultiphaseflow.2010.04.004.

[32] W. Jia, H.H. Qiu, Experimental investigation of droplet dynamics and heat transfer in spray cooling, Exp. Therm. Fluid Sci. 27 (2003) 829–838, https://doi.org/10.1016/S0894-1777(03)00015-3.

[33] H. Fujimoto, A.Y. Tong, H. Takuda, Interaction phenomena of two water droplets successively impacting onto a solid surface, Int. J. Therm. Sci. 47 (2008) 229–236, https://doi.org/10.1016/j.ijthermalsci.2007.02.006.

[34] A.Y. Tong, S. Kasliwal, H. Fujimoto, On the successive impingement of droplets onto a substrate, Numer. Heat Tran. Part A Appl. 52 (2007) 531–548, https://doi.org/10.1080/10407780701303716.

[35] G.V. Kuznetsov, N.E. Shlegel, Y. Solomatin, P.A. Strizhak, Combined techniques of secondary atomization of multi-component droplets, Chem. Eng. Sci. 209 (2019), 115199, https://doi.org/10.1016/j.ces.2019.115199.

[36] M.A. Clay, M.J. Miksis, M.A. Clay, M.J. Miksis, Effects of surfactant on droplet spreading, Phys. Fluids 16 (2004) 3070–3078, https://doi.org/10.1063/1.1764827.

[37] P. Pontes, E. Teodori, A.S. Moita, A.L.N. Moreira, U. De Lisboa, Time Resolved Infrared Analysis of Droplet Impacts onto Heated Surfaces under Extreme Wetting Scenarios, 2017, pp. 6–8, https://doi.org/10.4995/ILASS2017.2017.5012.

[38] S. Devireddy, C.S.R. Mekala, V.R. Veeredhi, Improving the cooling performance of automobile radiator with ethylene glycol water based TiO2 nanofluids, Int. Commun. Heat Mass Tran. 78 (2016) 121–126, https://doi.org/10.1016/j.icheatmasstransfer.2016.09.002.

[39] W.H. Mitrakusuma, S. Kamal, Indarto, M. Dyan Susila, Hermawan, Deendarlianto, The dynamics of the water droplet impacting onto hot solid surfaces at medium Weber numbers, Heat Mass Tran. 53 (2017) 3085–3097, https://doi.org/10.1007/s00231-017-2053-0.

[40] J.R. Taylor, An Introduction to Error Analysis, the Study of Uncertainties in Physical Measurement, second ed., University Science Books, Sausalito California, 1997.

[41] V. Mehdi-Nejad, J. Mostaghimi, S. Chandra, Air bubble entrapment under an impacting droplet, Phys. Fluids 15 (2003) 173–183, https://doi.org/10.1063/1.1527044.

[42] C. Bai, A.D. Gosman, Development of methodology for spray impingement simulation, SAE Tech. Pap. 950283 (1995) 69–87, https://doi.org/10.4271/950283.

[43] H.Y. Kim, J.H. Chun, The recoiling of liquid droplets upon collision with solid surfaces, Phys. Fluids 13 (2001) 643–659, https://doi.org/10.1063/1.1344183.

[44] H. Fujimoto, S. Ito, I. Takezaki, Experimental study of successive collision of two water droplets with a solid, Exp. Fluid 33 (2002) 500–502, https://doi.org/10.1007/s00348-002-0471-2.

[45] A. Riswanda, I. Pranoto, T. Wibowo, Deendarlianto, Indarto, Study on the effect of Weber Number to heat transfer of multiple droplets on hot stainless steel surface, 0–3, in: MATEC Web Conf., vol. 154, 2018, https://doi.org/10.1051/matecconf/201815401114.

[46] G.E. Cossali, M. Marengo, M. Santini, J. Watanabe, Secondary droplet atomisation from single drop impact on heated surfaces, in: ILASS Eur. 2002, 2002.

[47] G. Liang, S. Shen, Y. Guo, J. Zhang, Boiling from liquid drops impact on a heated wall, Int. J. Heat Mass Tran. 100 (2016) 48–57, https://doi.org/10.1016/j.ijheatmasstransfer.2016.04.061.

[48] N. Hatta, H. Fujimoto, K. Kinoshita, H. Takuda, Experimental study of deformation mechanism of a water droplet impinging on hot metallic surfaces above the Leidenfrost temperature, J. Fluids Eng. Tran. ASME 119 (1997) 692–699, https://doi.org/10.1115/1.2819300.

[49] H. Chen, W. Cheng, Y. Peng, L. Jiang, Dynamic Leidenfrost temperature increase of impacting droplets containing high-alcohol surfactant, Int. J. Heat Mass Tran. 118 (2018) 1160–1168, https://doi.org/10.1016/j.ijheatmasstransfer.2017.11.100.